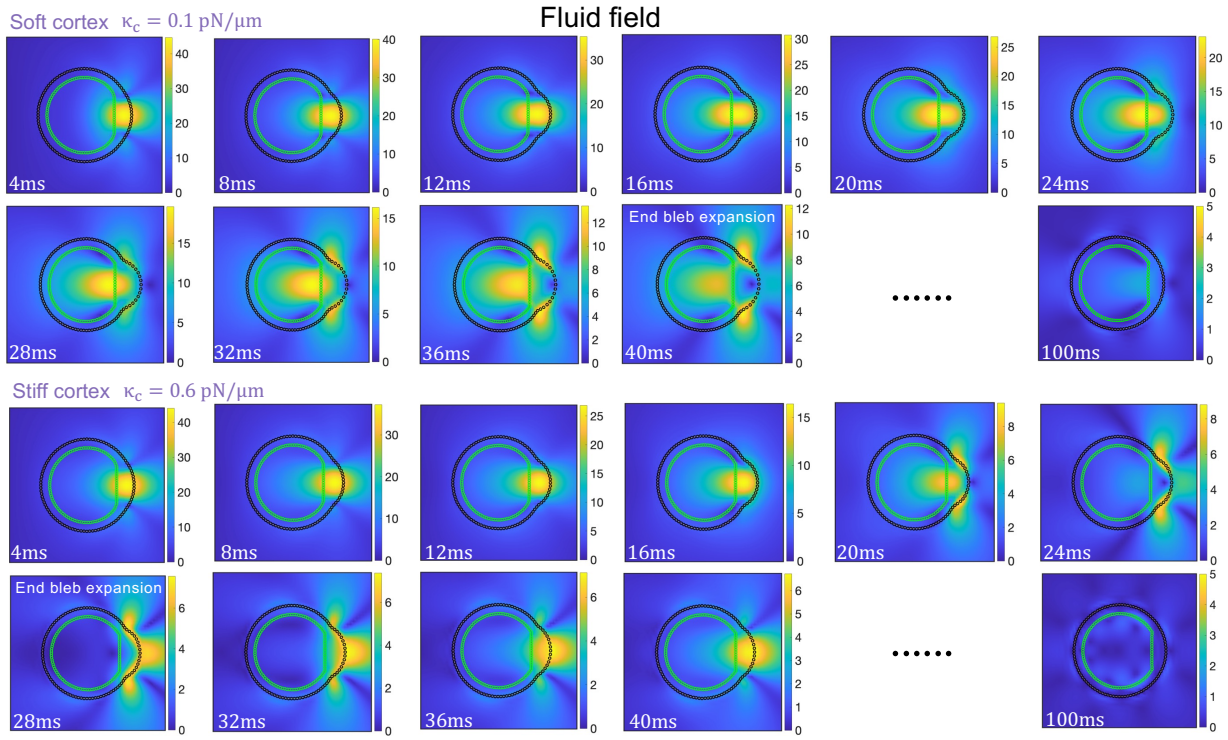

Figure S1A. Magnitude of the fluid field (μm/s) throughout a bleb cycle for two different values of the cortex stiffness per unit of actin parameter κ_c. Higher fluid velocities are observed for a softer cortex during both bleb expansion and bleb retraction. Membrane-cortex linkers are broken by hand locally in a small region at time $t = 0$, and are not allowed to break thereafter.

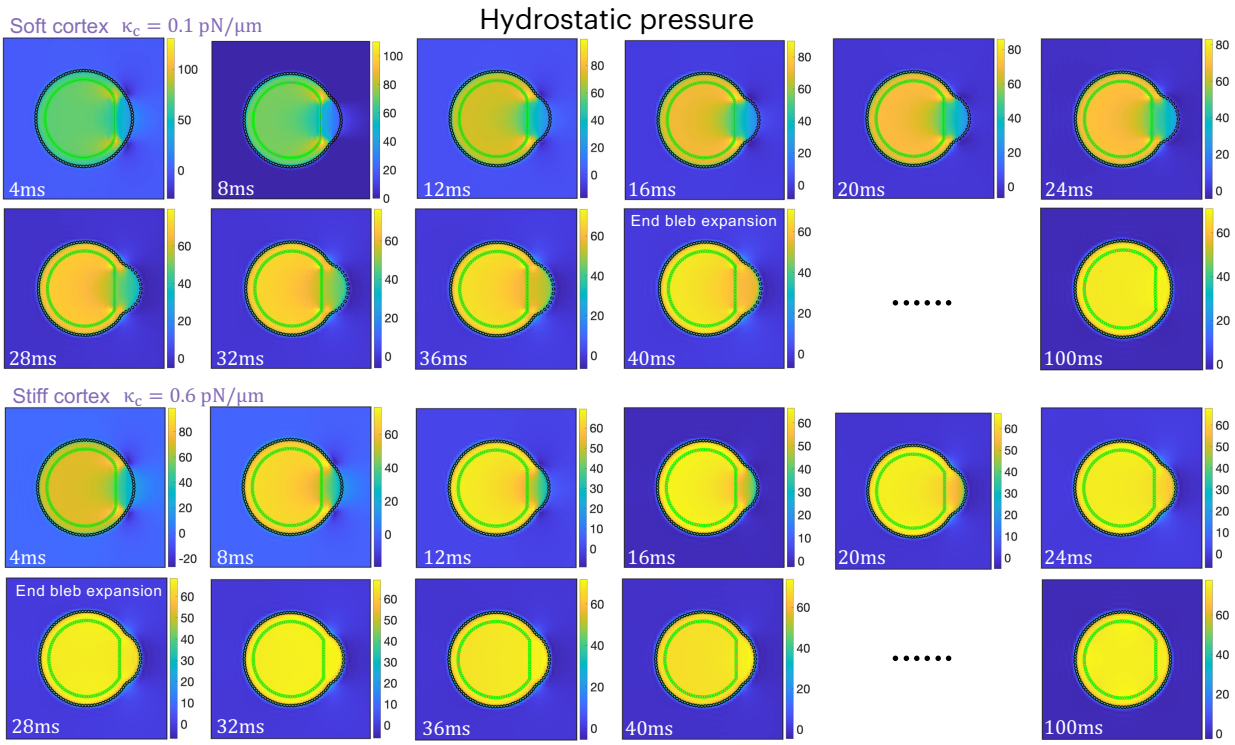

Figure S1B. Magnitude of the hydrostatic pressure (pN/μm) throughout a bleb cycle for two different values of the cortex stiffness per unit of actin parameter κ_c. Hydrostatic pressure equilibration and the end of bleb expansion occur at earlier times in the bleb cycle for a stiff cortex. Membrane-cortex linkers are broken by hand locally in a small region at time $t = 0$.

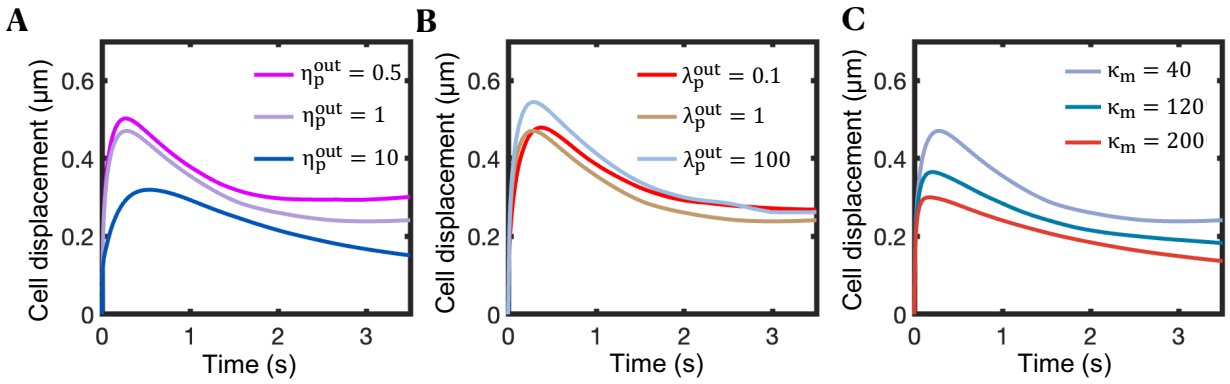

Figure S2. Cell displacements during a bleb cycle are influenced by extracellular and plasma membrane mechanical properties. (A–C) Time-evolution of the cell centroid for three different values of the cortex turnover parameter K_τ (A), three different values of the extracellular stress relaxation time λ_p^{out} (in seconds) (B), and three different values of the of the plasma membrane spring stiffness κ_m $(pN \cdot \mu m^{-1})$ (C). In all panels, membrane-cortex linkers are broken by hand locally in a small region at time $t = 0$, mimicking a local downregulation of membrane-cortex linkers due to a chemical signal or force. Unless otherwise specified, polymeric model parameter values: $\eta_p^{in} = 1\ pN \cdot s \cdot \mu m^{-1}$, $\lambda_p^{in} = 100\ s$, $\eta_p^{out} = 1\ pN \cdot s \cdot \mu m^{-1}$, $\lambda_p^{out} = 10\ s$.

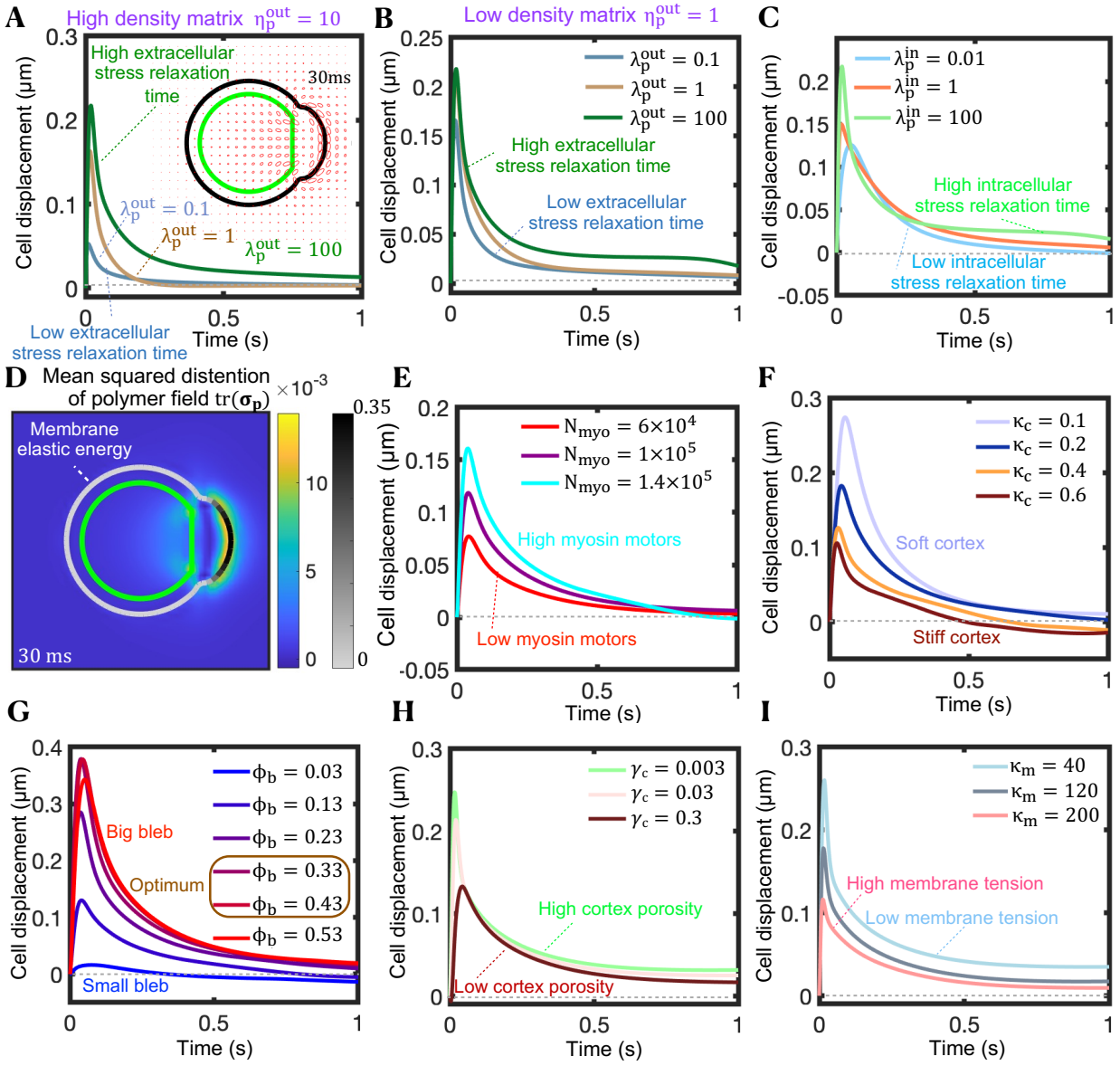

Figure S3. Net cell displacements for non-physiological fast turnover kinetics during a single bleb cycle are insignificant. (A,B) Time-evolution of the cell centroid for three different values of the extracellular stress relaxation time (in seconds) for high density matrix (A) and low density matrix (B). A short FENE-P stress relaxation time corresponds with a stiffer extracellular fluid. (A, inset) Ellipses represent the polymeric stress tensor $\boldsymbol{\sigma}_\mathbf{p}$ at a time-point during early bleb retraction. The major axis is aligned with the principal eigenvector of $\boldsymbol{\sigma}_\mathbf{p}$, with length scaled on the associated eigenvalue. The minor axis is associated with the second eigenvector of $\boldsymbol{\sigma}_\mathbf{p}$. The ellipses

represent the directions and distension of the polymer field. Elastic stresses build up at the cell front and resist pressure-driven bleb expansion. Unless otherwise stated, polymeric model parameter values: $\eta_p^{out} = 1\mathrm{pN}\cdot\mathrm{s}\cdot\mu\mathrm{m}^{-1}, \eta_p^{in} = 1\ \mathrm{pN}\cdot\mathrm{s}\cdot\mu\mathrm{m}^{-1},\ \lambda_p^{in} = 100\ \mathrm{s}$. (C) Time-evolution of the cell centroid for three different values of the intracellular stress relaxation time (in seconds). Polymeric model parameter values: $\eta_p^{out} = 0.1\mathrm{pN}\cdot\mathrm{s}\cdot\mu\mathrm{m}^{-1},\ \eta_p^{in} = 10\mathrm{pN}\cdot\mathrm{s}\cdot\mu\mathrm{m}^{-1},\ \lambda_p^{out} = 100\mathrm{s}$. (D) Mean-square distention of the immersed polymer material $\mathrm{tr}(\boldsymbol{\sigma_p})$ (blue-yellow scale bar) and local membrane elastic energy (gray-black scale bar) at a time-point during bleb retraction. Regions of high polymer stress and membrane elastic tension buildup at the cell front. (E–I) Time-evolution of the cell centroid for three different values of the number of myosin molecules inside the cell $\mathrm{N_{myo}}$ (E), for four different values of the cortical stiffness per unit of actin parameter κ_c (F), for different values of the fraction of the cell membrane perimeter (bleb size) ϕ_b that loses mechanical connection with the underlying cortex (G), for different values of the cortex-cytoplasm viscous drag coefficient $\gamma_c\ (\mathrm{pN}\cdot\mathrm{s}\cdot\mu\mathrm{m}^{-1})$ (H), and for different values of the plasma membrane spring stiffness $\kappa_m\ (\mathrm{pN}\cdot\mu\mathrm{m}^{-1})$ (I). High cortical contractility, soft cortex, intermediate bleb sizes, high cortex porosities and low plasma membrane stiffness maximize cell displacements during bleb expansion. In all panels, membrane-cortex linkers are broken by hand locally in a region set by ϕ_b at time $t = 0$. Cortex turnover parameter value: $K_\tau = 100$.

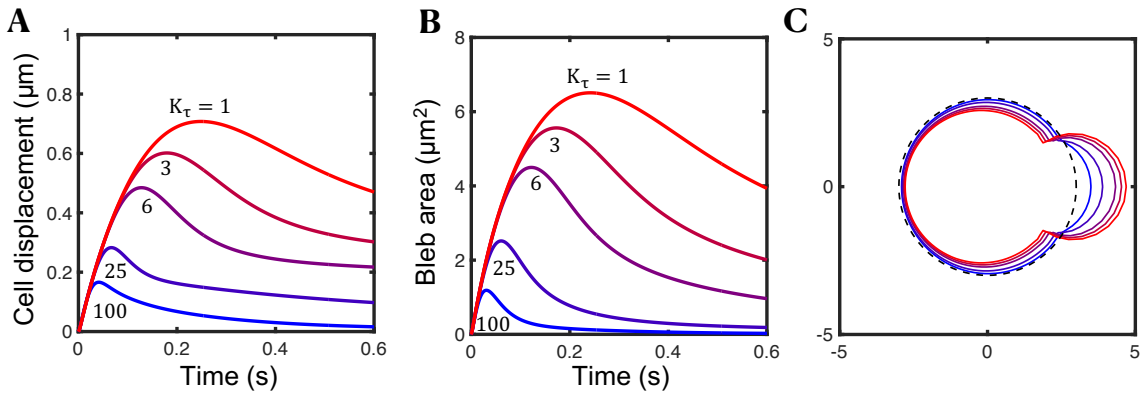

Figure S4. Cortex turnover regulates bleb retraction dynamics. (A–C) Time-evolution of the cell centroid (A), time-evolution of the bleb area (B) and cell shape at maximum bleb area (C) for five different values of the cortex turnover factor K_τ. Extracellular and intracellular spaces are considered Newtonian fluids.

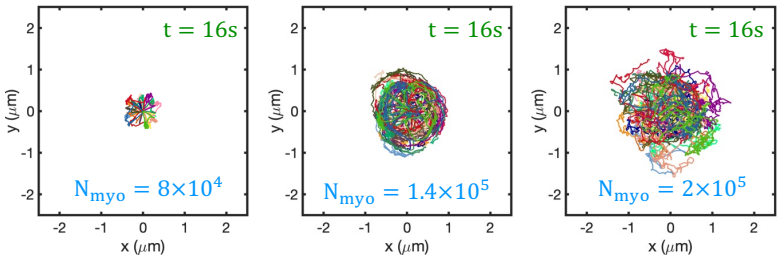

Figure S5. High contractile bleb-producing cells swim more efficiently. Wind rose plots depicting the migratory tracks of cells for three different myosin levels: low (left), intermediate (center), high (right). Each color represents a single-cell trajectory. Intermediate myosin levels ($N_{myo} = 1.4 \times 10^5$) build up a hydrostatic intracellular pressure of ~50 pN/μm (see Fig. S1B), comparable to that of T cells under DMSO conditions [21].

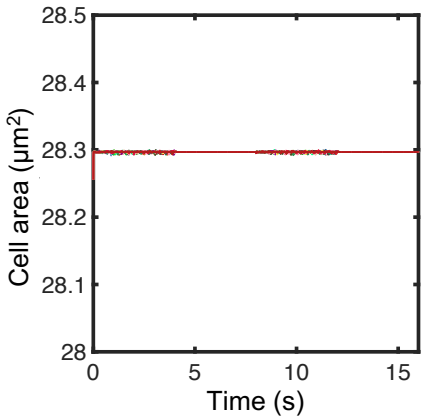

Figure S6. Time evolution of cell area for all the cells in Fig. S5 (center). Throughout the simulations, the cell area remains conserved.

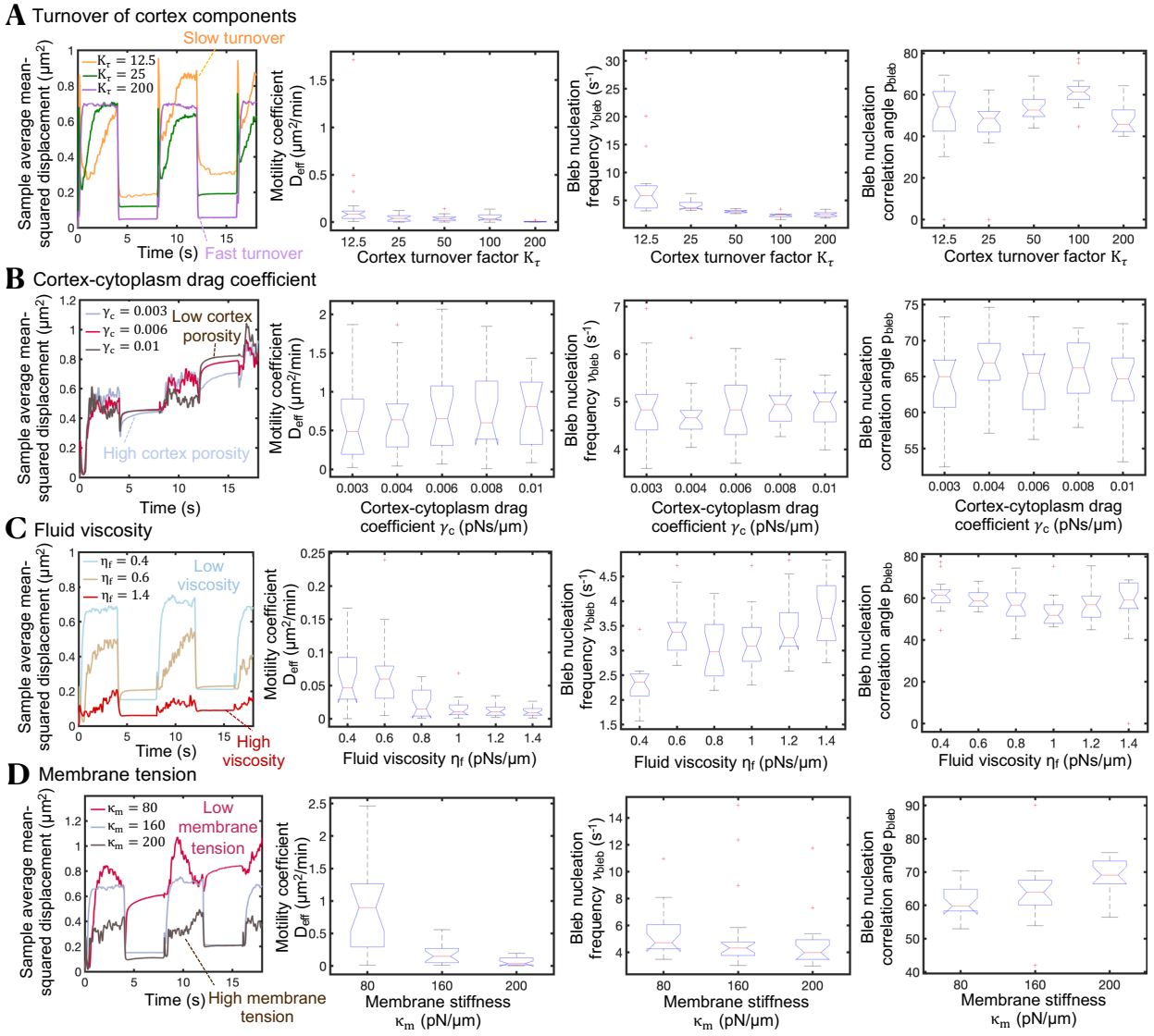

Figure S7. Cortex turnover, cortex porosity, fluid viscosity and membrane tension modulate bleb-based cell swimming capabilities. (A–D) Sample average mean-squared displacement, random motility coefficient $\mathrm{D_{eff}}$, bleb nucleation frequency ν_{bleb}, and polar angle between consecutive bleb nucleation events $\mathrm{p_{bleb}}$ for different values of the (A) cortex turnover factor $\mathrm{K_\tau}$, (B) cortex-cytoplasm drag coefficient γ_c $(\mathrm{pN \cdot s \cdot \mu m^{-1}})$, (C) fluid viscosity η_f $(\mathrm{pN \cdot s \cdot \mu m^{-1}})$ and (D) membrane spring stiffness parameter κ_m $(\mathrm{pN \cdot \mu m^{-1}})$.

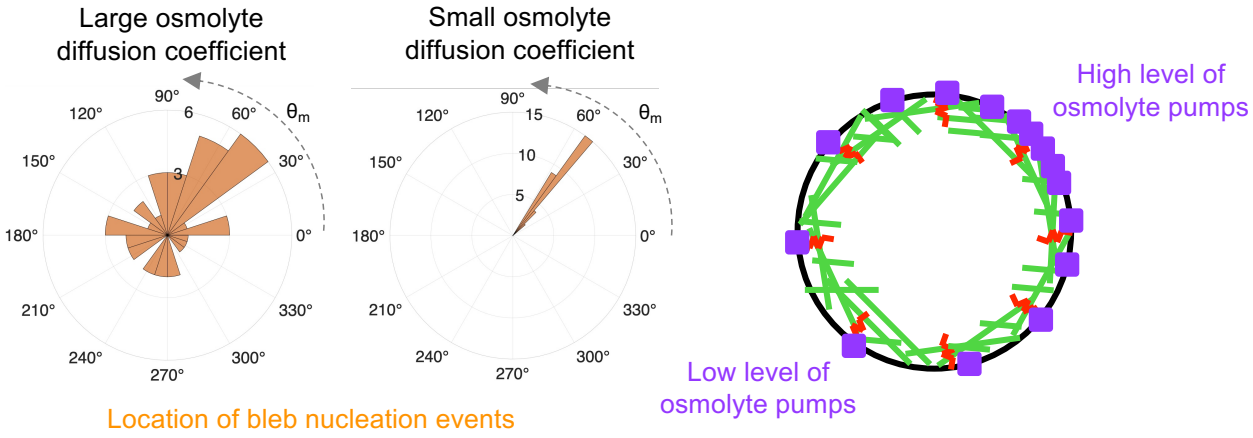

Figure S8. Blebs nucleate in high osmotic pressure regions. (A) Polar distribution of bleb nucleation events for fast osmolyte diffusion ($D_{in} = 500\mu m^2/s$) and slow intracellular osmolyte diffusion ($D_{in} = 5\mu m^2/s$), for an asymmetric osmolyte active pumping influx $\alpha_{pump}(s_j, t) = 10^7 \sin\theta_{m_j} \cos\theta_{m_j}$, where θ_{m_j} is the polar angle associated to the jth membrane node. Parameter values: $D_{out} = 2D_{in}$ and $\alpha_{passive} = 10^{-3}$.

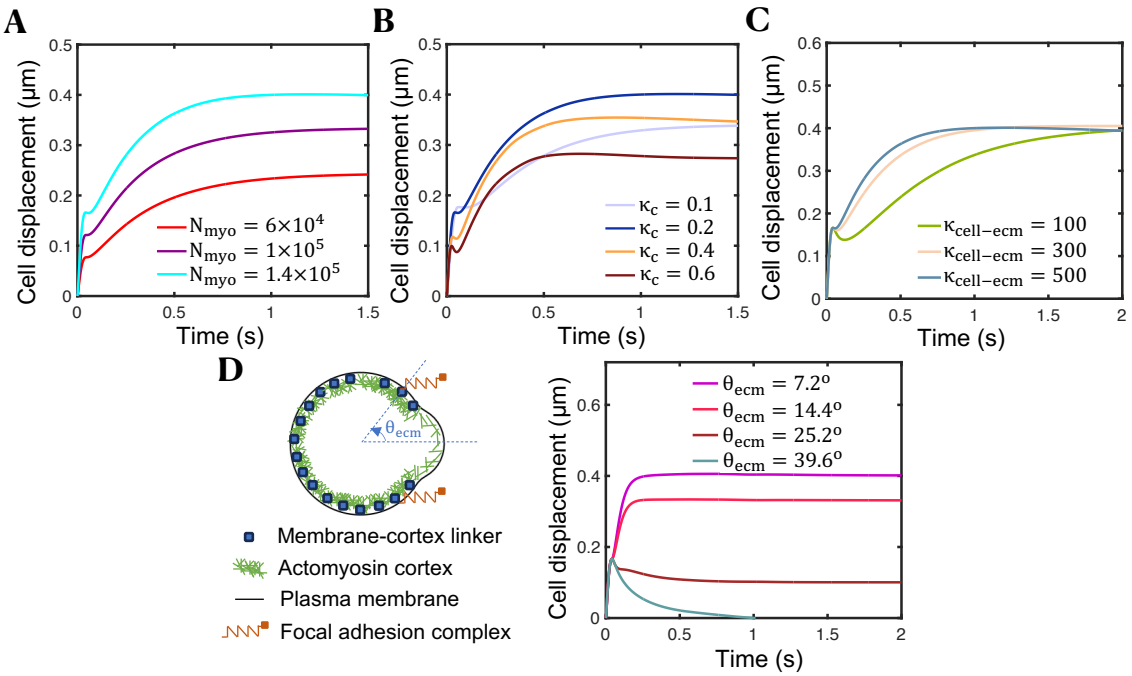

Figure S9. Substrate stiffness does not impact cell displacements in the hybrid adhesion-bleb migration mode. (A–C) Time-evolution of the cell centroid for three different values of the number of myosin molecules inside the cell N_{myo} (A), four different values of the cortical stiffness per unit of actin parameter κ_c (B), and for three different values of the effective stiffness of the cell-extracellular matrix tandem $\kappa_{cell-ecm}$ (C). Larger cell displacements are achieved for elevated cortical tensions and intermediate cortical stiffnesses levels. (D) Time-evolution of the cell centroid for four different configurations of cell-matrix adhesion complex formation. Greater cell displacements are achieved when adhesions form at the cell's front. Notice that the inclusion of two focal adhesions can mimic the squeezing of cells through narrow pores.

Movie S1: Fluid field (left), hydrostatic pressure (middle) and temporal evolution of cell displacements (right) during a single isolated bleb cycle in the absence of adhesion-based forces. Velocity field is expressed in $\mu m/s$ and hydrostatic pressure in $pN/\mu m$.

Movie S2: Representative migration dynamics of a cell in the absence of cortical oscillations. Colors and vectors represent the magnitude and directionality of the fluid velocity (in $\mu m/s$).

Movie S3: Cortex and plasma membrane dynamics (left) and temporal evolution of cell displacements (right) during a single isolated bleb cycle in the presence of adhesion-based forces.